

194086  
33P

**NASA Technical Memorandum 109000**

**Packaging, Deployment, and Panel Design Concepts for a Truss-Stiffened 7-Panel Precision Deployable Reflector with Feed Boom**

**Walter L. Heard, Jr., Timothy J. Collins, James W. Dyess, W. Scott Kenner and Harold G. Bush**

**November 1993**

(NASA-TM-109000) PACKAGING,  
DEPLOYMENT, AND PANEL DESIGN  
CONCEPTS FOR A TRUSS-STIFFENED  
7-PANEL PRECISION DEPLOYABLE  
REFLECTOR WITH FEED BOOM (NASA)  
33 P

N94-17765

Unclas

G3/18 0194086



National Aeronautics and  
Space Administration

**Langley Research Center**  
Hampton, Virginia 23681-0001



# Packaging, Deployment, and Panel Design Concepts for a Truss-Stiffened 7-Panel Precision Deployable Reflector with Feed Boom

by

Walter L. Heard, Jr., Timothy J. Collins, James W. Dyess, W. Scott Kenner, and  
Harold G. Bush

## Abstract

A concept is presented for achieving a remotely deployable truss-stiffened reflector consisting of seven integrated sandwich panels that form the reflective surface, and an integrated feed boom. The concept has potential for meeting aperture size and surface precision requirements for some high-frequency microwave remote sensing applications. The packaged reflector/feed boom configuration is a self-contained unit that can be conveniently attached to a spacecraft bus. The package has a cylindrical envelope compatible with typical launch vehicle shrouds. Dynamic behavior of a deployed configuration having a 216-inch focal length and consisting of 80-inch-diameter, two-inch-thick panels is examined through finite-element analysis. Results show that the feed boom and spacecraft bus can have a large impact on the fundamental frequency of the deployed configuration. Two candidate rib-stiffened sandwich panel configurations for this application are described, and analytical results for panel mass and stiffness are presented. Results show that the addition of only a few rib stiffeners, if sufficiently deep, can efficiently improve sandwich panel stiffness.

## Introduction

In support of NASA's Mission to Planet Earth program, space-based observation systems are needed for scientific monitoring of Earth system processes (refs. 1, 2). For some applications such observation systems (spacecraft) will require parabolic reflectors with diameters that exceed shroud diameters of practical launch vehicles. Thus, if manned and robotic assembly of erectable structures are not considered affordable options for near-term applications, these reflectors must be assembled on Earth, folded for launch and remotely deployed on-orbit. This requirement significantly increases structural complexity and introduces reliability issues that must be addressed by the designer. An additional design complication arises from the fact that an application of major interest for remote sensing spacecraft is microwave radiometry at frequencies greater than 30 GHz. At these high frequencies expandable mesh becomes inadequate as a reflective surface and must be replaced by a solid reflective surface (ref. 3). If the reflective surface must also be stiffened to meet high precision requirements, compact packaging becomes even more difficult to achieve than for mesh surfaces.

Reference 4 presents a concept for packaging and deployment of a reflector with a stiffened reflective surface that is supported on a truss. The concept achieves high volumetric packaging efficiency by dividing the reflective surface into smaller panel segments that can be arranged in a compact stack so that the package fits within a cylindrical envelope compatible with launch vehicle shrouds. This concept has the potential for achieving high precision, and, using a launch vehicle having a shroud diameter similar to that

of the Space Shuttle cargo bay (15 ft), a reflector with a 33 ft aperture is possible. Integration of a feed boom, however, is not addressed in reference 4

The primary objective of the present study is to expand the conceptual ideas presented in reference 4 by devising a different deployment concept for a seven-panel reflector and include integration of a feed boom while maintaining the cylindrical package envelope. The dynamic behavior of this reflector concept in its deployed configuration is also examined through finite-element analysis to assess the effects of the feed boom, feed mass, and spacecraft bus mass. A configuration having a 216-inch focal length and consisting of 80-inch-diameter panels is selected for this study. The focal length selected for the analytical model dictates a relatively long feed boom that probably approaches an upper limit for the reflector concept presented herein. Details of the actuators, zero-play hinge joints, and other hardware required to withstand launch loads and effect deployment are not included in this paper. Finally, two configurations for lightweight solid-surface panels are presented with the goal of identifying panel concepts that meet the weight, surface accuracy, and packaging (for launch) requirements of remote sensing small spacecraft.

#### Design Considerations

Because the reflector concept devised herein does not have a specific mission, loads and performance requirements are not available. However, microwave radiometry at high frequencies requiring an accurate, stiffened, solid reflective surface is assumed to be the primary mission that will influence structural considerations for the deployed configuration. The following guidelines are used to configure the reflector concept considered herein:

1. The reflector should be an offset-fed configuration with an integrated deployable feed boom.
2. The reflector surface should be segmented into sufficiently small, similar-size, stiffened, hexagonal panels to enable efficient packaging in practical-size launch vehicles.
3. The packaging and deployment scheme should accommodate curved panels.
4. Each panel should be supported on three flexures following deployment (deployment mechanisms should not remain in the load paths) to reduce the effects of the interaction of mechanical and thermal distortions between the panel and the truss.
5. The reflector and integrated feed boom should be compatible with attachment to a spacecraft bus.
6. The relative geometrical positions of appropriate structural nodal points in the support truss should not change during deployment, thus providing convenient attachment points by which the reflector package can be attached, as a unit, to a spacecraft bus.

### General Configuration and Packaging Scheme

The configuration assumed for the reflector concept studied herein is shown in figure 4. The integrated reflector and feed boom package is attached to one end of a spacecraft bus and deployed when the desired orbit is achieved. The reflector has an offset feed and the reflective surface is composed of seven stiffened, similar-size, hexagonal-shaped panels that are supported by a truss. As shown in figure 2, the support truss has a non-deployable center section, referred to herein as the center-body truss, and six deployable truss wings. The non-deployable center-body truss, which supports the center panel, also provides a simple and convenient interface for attachment of the reflector package as a unit to the spacecraft bus. The truss wings, which when folded lie parallel to the axis of the spacecraft bus (see fig. 1 (a)), deploy independently of each other, and one linear actuator is required to deploy each wing. (Additional actuators are required to position the panels--a significant complexity that requires some design ingenuity to conserve volume as well as mass.) The perspective view in figure 2 shows the center panel, the center-body truss, and one of the truss wings with its corresponding panel in the deployed position. The actuator motions required to deploy or restow the reflector are shown in the enlarged perspective view in figure 3. The center panel, which does not deploy, is permanently supported over the center-body truss at three equally spaced peripheral points located at the midpoints of every other edge of the panel (fig. 2). Flexural supports are used to attach the center panel to the appropriate nodes of the center-body truss to permit essentially free in-plane thermal expansion. Each of the six outer panels must also ultimately be supported on three flexures--one each at the two outboard nodes of a deployable truss wing and a third at the corresponding inboard node on the center-body truss. The translational motion of an outer panel in the plane of the panel (indicated in figure 3 by the gray arrow), may not be necessary. If the length of the longest member in the truss wing (which, when folded, lies normal to the diametrical plane of the center panel and is nominally equal to the length of the packaged reflector plus the spacecraft bus length) is not restricted by the launch vehicle shroud length, the wing can be extended radially to permit support of the panel at its two outermost corners.

The packaged configuration for the reflector and feed boom is shown schematically in figure 4. An exploded view of the deployed configuration is shown schematically in figure 5. The main components are the support truss, the seven reflector panels, the feed boom, and the transition truss which is used to connect the feed boom to one of the truss foldable wings. As seen in figure 4(b), the diameter of the package is slightly larger than the diameter of the panel stack. Because the reflector is an offset paraboloid, each of the panels has unique dimensions. However, for most applications the panels can probably be designed such that their planform dimensions are sufficiently similar to cause no significant effect on the diameter of the cylindrical package envelope. When the wings are folded, the outboard panels stack over the center panel, with the concave sides all facing in the same direction.

The feed boom consists of multiple, straight, truss-beam segments that are connected end-to-end by hinge joints. The hinge joints allow 180° rotation such that, in the stowed configuration, the segments are parallel and contiguous with connecting segments. The required number of hinge joints depends on the focal

length of the parent paraboloid and the diameter of the panels in the reflector dish. Only two of the feed boom hinge joints are shown in figure 5-- one at the interface with the transition truss and the other at the "elbow" of the feed boom. The axes for these two hinge joints are mutually perpendicular. In addition, the feed boom segments must not have protrusions that would significantly compromise the tightness of the package. The length of each segment is limited to the approximate distance between opposite edges of the panels as shown in figure 4(a). It is assumed that the articulated-truss joint concept proposed for space crane application, and designated "A" in reference 5, can be miniaturized for application as the feed boom hinge joints. The articulated truss joint concept chosen is shown in figure 6.

### Deployment Sequence

The basic sequence of motions necessary to deploy the reflector and feed boom is shown in figure 7. Design details of the required linkages, actuators, fittings, and latches to cause these motions, maintain the proper deployed configuration, and support the packaged for survival of launch loads are not addressed in this study.

The initial step in deploying the reflector is to rotate the transition truss (with attached feed boom) to a position outside the package envelope. The transition truss is hinged at its outboard edge to the outboard edge of one of the truss wings (see fig. 5). There are two latch fittings at the inboard edge of the transition truss that connect to corresponding fittings at the base of the truss wing (at the center-body truss) when the 270 degree rotation is completed. In the second step, the top panel is translated to the top of the package and the feed boom is rotated 180 degrees. These positions allow the first truss wing (with attached panel and transition truss) to be deployed, as shown in step 3 in figure 7, without interference from adjacent structure or the spacecraft bus. The first panel is then rotated and translated, as shown in step 4, to its final position. The other five truss wings and corresponding panels are deployed in a similar manner (omitting the manipulations of the feed boom and transition truss). Deployment of the feed boom, as shown in the remainder of figure 7, can be completed at any time following deployment of the first truss wing and panel. If the first three panel wings deployed are non-adjacent, the threat of obstruction from adjacent structure is removed for the remaining three panels so that simplified mechanisms may be possible for their deployment.

Although the reflector concept presented herein is packaged in a cylindrical envelope for compatibility with cylindrical shrouds of standard expendable launch vehicles, the deployment sequence proposed is compatible with a flight verification experiment for which the cylindrical package could be launched mounted transversely in the Space Shuttle on a Hitchhiker Bridge Assembly (HHBA) as indicated in figure 8. The HHBA is the pallet used for the Hitchhiker carrier system (ref. 6). The Hitchhiker carrier system provides the power and data link needed to control deployment and repackaging. A remote repackaging capability is required for a Shuttle-launched flight experiment designed for multiple remote deployments to demonstrate deployment reliability. A repackaging capability is also required to return the reflector to Earth

in the Shuttle. A repackaging requirement complicates the structure by requiring joints that lock in the deployed configuration to have an unlocking capability. Locks on the ancillary structure required to withstand launch loads would also require a remote locking and unlocking capability. For the present study, it is assumed that solenoids or small electric motors can be incorporated on the joints to perform this function. In addition, the actuator motions required to effect the deployment sequence (see figure 7) are assumed to be reversible to enable repackaging of the reflector.

### Support Truss Geometry

The general configuration of the support truss for the reflector concept presented herein is devised so that each of the six wings of the truss can be deployed, independently, by separate linear actuators. The dimensions of the support truss are determined from the equations and procedure presented in this section.

The truss geometry is defined in figure 9. The depth of the center-body truss must be sufficient to enable vertical folding of the truss wings. In addition, the corner-to-corner diameter of the base of the center-body truss must be similar to the nominal corner-to-corner diameter of the panels. Finally, the corner-to-corner diameter of the upper surface of the center-body truss must be similar to the nominal distance between opposite edges of the panels (see fig. 2).

The truss wing is shown in the folded position in figure 9(a) and in the deployed position in figure 9(b). For deployment, a linear actuator is used to move point A (fig. 9(a)) vertically upward until point A becomes coincident with point B (fig. 9(b)). To make it possible for the actuator to deploy the truss wing the angle,  $\beta$ , must be greater than zero; thus hinge line offset,  $e_1$ , must be less than the hinge line offset,  $e_2$ . (The hinge lines are perpendicular to the plane of figure 9, and are represented by the small circles at the ends of projected member  $S_1$  and member  $S_2$ .) The specific value of  $e_2$  will effect the diameter of the packaged reflector and, thus, should be chosen as small as practical with consideration given to maintaining a practical value of  $e_1$  and providing sufficient mechanical advantage for the actuator to operate effectively. The offset  $e_3$  is also specified with consideration given to maintaining a practical distance between the members in the base of the center-body truss and the hinge line at the lower end of projected member  $S_1$  (with the truss wing is in the folded position).

The diameter of the envelope of the reflector package (nominally, the diameter of the panels plus an amount to account for the  $e_2$  offsets and cross-sectional dimensions of the  $S_2$  members) is selected to match the diameter of the dynamic envelope of the launch vehicle shroud. The depth of the package envelope must also be compatible with the launch vehicle shroud as well as provide sufficient volume above the center-body truss to contain the panel stack, the feed boom, and the transition truss (fig. 9(a)). The center-body truss depth depends on the length of travel required for the linear actuator to fold the truss wing from the deployed position shown in figure 9(b) to the position where member  $S_2$  is vertical (fig. 9(a)). (In figure 9(b) projected member  $S_1$  is parallel to the chord connecting points  $(x_1, z_1)$ , and  $(x_2, z_2)$  on the parent paraboloid generator.)

Although the reflector is an offset paraboloid, an axisymmetric reflector is assumed for purposes of defining the angle  $\alpha$  of projected member  $S_1$  (fig. 9(b)). Thus, the center of the center panel surface is assumed to lie at the vertex of the parent paraboloid. (This simplifying assumption should have little effect on the dynamic analysis results presented in the following section.) For ease of fabrication, the support truss would probably be an axisymmetric structure even for an offset reflective surface, so that the inclinations of the truss wings would all be equal. The panel support flexures would be of various lengths to account for the asymmetry of the reflector surface panels.

The geometric parameters of the support truss are determined as follows:

The angle  $\alpha$  is given by

$$\alpha = \tan^{-1} \frac{(z_2 - z_1)}{(x_2 - x_1)} \quad (1)$$

and

$$x_1 = \frac{D_f}{2} \quad (2)$$

$$z_1 = \left( \frac{D_f}{2} \right)^2 \frac{1}{4F} \quad (3)$$

$$z_2 = \frac{x_2^2}{4F} \quad (4)$$

where  $D_f$ , the edge-to-edge diameter of the panels and  $F$ , the focal length, are known.

The value of  $x_2$  can be determined by substituting eqs. (2), (3), and (4) into the equation

$$D_f^2 = (x_2 - x_1)^2 + (z_2 - z_1)^2$$

to obtain

$$C_1 x_2^4 + C_2 x_2^2 + C_3 x_2 + C_4 = 0 \quad (5)$$

where

$$C_1 = \frac{1}{16F^2}; \quad C_2 = 1 - \frac{1}{32} \left( \frac{D_f}{F} \right)^2; \quad C_3 = -D_f; \quad (6)$$

$$C_4 = D_f^2 \left[ \frac{1}{256} \left( \frac{D_f}{F} \right)^2 - \frac{3}{4} \right]$$

Equation (1) can now be solved for the angle  $\alpha$ .



From figure 9, the depth of the package can be expressed as

$$H_p = S_2 + e_2 \tan \theta + \frac{ds}{2} \quad (7)$$

where  $ds$  is the diameter of the struts in the base of the center-body truss. The other geometric relations that must be satisfied to fold the truss wing to the position shown in figure 9(a) are:

$$\sin \beta = \frac{e_2 - e_1}{S_1} \quad (8)$$

$$\theta = \cos^{-1} \left( \frac{S_1 \cos \alpha + e_1 - e_2}{S_2} \right) \quad (9)$$

$$S_2 = e_3 + S_1 \sqrt{1 - \sin^2 \beta} \quad (10)$$

Eqs. (8) and (10) can be combined to obtain

$$S_1 = \sqrt{(S_2 - e_3)^2 + (e_2 - e_1)^2} \quad (11)$$

and combining eqs. (7) and (9) yields

$$H_p = S_2 + e_2 \left\{ \frac{\sqrt{S_2^2 - (S_1 \cos \alpha + e_1 - e_2)^2}}{(S_1 \cos \alpha + e_1 - e_2)} \right\} + \frac{ds}{2} \quad (12)$$

With  $\alpha$ ,  $e_1$ ,  $e_2$ ,  $e_3$ ,  $ds$ , and  $H_p$  known, an iterative process is used to determine corresponding values of  $S_1$ ,  $S_2$ ,  $\theta$ , and  $\beta$ . The center-body truss depth,  $h_t$ , can then be calculated by

$$h_t = S_2 \sin \theta - \left( S_1 + \frac{e_1}{\cos \alpha} \right) \sin \alpha + e_2 \tan \theta$$

#### Dynamic Analysis of Deployed Reflector

To gain an understanding of the dynamic behavior that can be expected for a deployed reflector configuration such as described herein, a representative reflector having a focal length,  $F$ , of 216 inches and composed of 80-inch-diameter panels was selected for analysis. To determine the truss geometry it is assumed that the reflector would be launched mounted to a HHBA aboard the Space Shuttle, as shown in figure 8. For this case, the axis of the reflector package is perpendicular rather than parallel to the longitudinal axis of the launch vehicle. Thus, the depth of the package is the critical dimension that must be restrained so that the package does not penetrate the Shuttle dynamic envelope (fig. 8(a)). A package depth of 50 inches was specified. This depth allows space for ancillary structure (fig. 8(b)) of hexagonal

cross-section that simulates the spacecraft bus cross section. The ancillary structure also serves as an interface between the relatively narrow MPESS and the reflector package. The resulting support truss has an 8.9-inch-deep center-body truss and, with the wings folded, provides enough space above the center-body truss to accommodate the stack of seven 2-inch-thick panels with a 0.5 inch spacing, a feed boom having an 8-inch-square cross-section, and a transition truss that is 6 inches deep. However, the package depth is constrained such that the truss wings are too short to support the outer panels at their two outermost corner points. Thus, a translational motion in the plane of each outer panel is required to place it in its final deployed position.

Finite-element model.- A finite element model was created and analyzed using the EISI-EAL computer code (ref. 7). The model, shown in figure 10, consists of the non-deployable center-body truss, 6 deployable truss wings, the transition truss, and the feed boom (see fig. 5). The structure is assumed to consist of graphite-epoxy members having a modulus of elasticity of  $40 \times 10^6$  psi and a mass density of 0.06 lbm/in<sup>3</sup>. All members except the two tension members in each truss wing are 0.5 inches in diameter. The tension members, which are included to provide shear stiffness to truss wings, are 0.125 inches in diameter. The longeron and diagonal members in the root segment of the feed boom (the shorter straight segment of the feed boom that connects to the transition truss), the transition truss, the wing supporting the transition truss, and the tension members are modeled as solid rods. All other members are modeled as hollow tubes with a wall thickness of 0.02 inches. (The replacement of selected tubular members with solid members in the model was found to be most effective in raising the fundamental frequency of the structure as a whole.) To reduce the mass of the long portion of the feed boom and improve dynamic behavior, bays twice as long as cubic bays are modeled. This modeling does not reduce the bending stiffness of the feed boom and maintains adequate torsional stiffness to preclude a critical torsional mode for the range of offset feed masses investigated. Only two of the articulating joints in the feed boom are modeled--those at each end of the feed boom root section. With these assumptions, the structural mass of the center-body truss, wings, transition truss, and feed boom is 28.5 lbm. All members of the center-body truss and truss wings are divided into 4 beam elements each. In addition, the 15 longest members of the transition truss are divided into 2 beam elements each. These members are subdivided in order to determine local vibration modes. The entire model consists of 380 nodes (2280 degrees of freedom) and 576 beam elements.

The nodal joints (the points where two or more of the truss members interconnect) in the support truss and in the feed boom are modeled as lumped (non-structural) masses. Furthermore, all of these nodal joints are assumed to have identical masses. If a nodal joint also supports an actuator, the nodal joint mass is increased accordingly. The panels are also modeled as lumped masses that are apportioned to the respective support nodes in the truss. (The value assumed for the mass of a panel is estimated from design curves for the lightweight, solid-surface panel designs presented in the next section of the present paper.) Finally, a lumped mass representing the feed is located 8 inches from the free end of the feed boom and

offset 12 inches from its longitudinal axis toward the reflector side. The masses assumed for the various components are listed in Table 1.

The deployable reflector package will most likely be attached to a spacecraft bus of significant mass for a given mission. To account for this, the spacecraft bus is assumed to be a lumped mass located on the longitudinal axis of the reflector and offset 25 inches from the base of the center-body truss. The mass is assumed to be connected by three rigid members to three equally spaced nodes located on the periphery of the base of the center-body truss.

Analytical results.- Because the present reflector concept does not have a specific mission, the feed mass and the spacecraft bus mass are unknown. However, it is assumed that the mass of a feed for a reflector of the size being analyzed would not exceed 20 lbm, and that the mass of the spacecraft would not exceed 1400 lbm. Table 2 presents the fundamental and second lowest natural frequencies for selected values of feed and spacecraft bus masses. The mode shapes associated with these frequencies are indicated in Table 2 by (T) or (B). Although the mode shapes for the two lowest natural frequencies are complex, they are referred to herein as either a twisting mode (T) or a bending mode (B) because these terms are somewhat descriptive of the vibratory motion. Typical examples of these mode shapes are shown in figure 11. The twisting mode, which is shown in figure 11(a), is characterized by bending and torsion of the long section of the feed boom and torsion of the root section of the feed boom, causing a twisting of the transition truss, the wing, and, consequently, the center-body truss. The bending mode, which is shown in figure 11(b), is primarily bending of the feed boom toward and away from the center-body truss.

The effect of feed mass and spacecraft bus mass on fundamental frequency is shown graphically in figure 12. In this figure fundamental frequency is plotted as a function of feed mass for various values of spacecraft bus mass. When the feed mass and the spacecraft bus mass are both zero, the fundamental frequency is about 8.4 Hz. Comparing this value with the fundamental frequency of 25.6 Hz obtained for the reflector when the feed boom and associated support structure are removed from the model demonstrates the dominant effect of the feed boom on fundamental frequency. In figure 12 the frequency is seen to decrease with increasing feed mass. For the case of zero spacecraft bus mass, the fundamental frequency is reduced by 37% when the feed mass is increased from 0 to 20 lbm. The results in figure 12 also show that increasing spacecraft bus mass further decreases fundamental frequency. As the spacecraft bus mass is increased, the boundary conditions on the spacecraft bus end of the structure (at the base of the center-body truss) approach a clamped condition for which the fundamental frequency is shown by the hatched line in figure 12. A Space Shuttle flight experiment wherein the deployed reflector would remain firmly attached to a support pallet in the cargo bay would experience this degradation in fundamental frequency.

The structure can be modified to effect small increases in the fundamental frequency. For example, changing the center-body truss to all solid members increases the fundamental frequency approximately 7%, but increases the total structural mass by 51%. The truss wings might also be structurally reconfigured to gain some increase in stiffness. Recall that the packaged reflector has a hexagonal cross section, thus there

is some space available inside the cylindrical package envelope which could be used for structural stiffening purposes. However, such structural modifications would compete for the available space with any ancillary structure required to support the package in an expendable launch vehicle for survival of launch loads.

### Reflector Panel Design and Analysis

As part of the effort to develop enabling technologies for precision deployable reflector systems, several lightweight, solid-surface panel designs are being investigated with the goal of identifying panel concepts that meet the weight, surface accuracy, and packaging (for launch) requirements of remote sensing micro-spacecraft. The primary panel performance parameters are expected to be weight, stiffness, and surface accuracy. A major emphasis of the design process is to fabricate panels having minimum weight and maximum stiffness and meeting specified surface accuracy requirements. Also, it is necessary to satisfy packaging requirements for launch and to consider limitations related to cost and panel fabrication. This section presents analysis results related to panel mass and stiffness for the two panel stiffener configurations shown in figure 13. Examination of issues related to panel fabrication, cost, and on-orbit surface accuracy is ongoing, but is beyond the scope of this paper.

One possible panel design, shown in figure 13, utilizes a sandwich construction consisting of two thin high-modulus graphite-epoxy face sheets separated by a lightweight honeycomb core. An arrangement of rib stiffeners is bonded to the convex face of the panel (the non reflective face). The stiffeners improve design efficiency by increasing panel stiffness without a significant increase in panel mass. The stiffeners, also of a sandwich construction, are designed to have a coefficient of thermal expansion (CTE) that is approximately equal to that of the sandwich panel. A variety of commercially available graphite-epoxy material systems can be used to fabricate the face sheets. Aluminum and several low-CTE non-metallic materials are being considered for the honeycomb core of both the panel and stiffeners.

A cross-sectional view of a typical panel-stiffener arrangement is shown in figure 14. Analysis results presented in this section were obtained for panels having a flat (no curvature) surface as shown in figure 14. Although the panel surface will actually be doubly curved (generally parabolic), it has been found that analysis results are not strongly dependent upon panel curvature for moderately curved reflectors. The face sheets are fabricated from a high-modulus graphite-epoxy material system. For the present study, each facesheet uses four plies to produce a  $[0^\circ/\pm 45^\circ/90^\circ]$  laminate. Two such face sheets, when bonded to the panel core, yield a sandwich panel with quasi-isotropic material properties. The face sheet laminates are assumed to have an in-plane Young's modulus of approximately  $15 \times 10^6$  psi and a density of  $0.065 \text{ lbm/in}^3$ . The panel core assumed here is a low-modulus aluminum honeycomb material having a density of  $1.5 \text{ lbm/ft}^3$ . This core has approximately the lowest density that can be obtained using either aluminum or non-metallic honeycomb core material. Both the in-plane and shear moduli of the core are low. The core serves primarily to add depth (and hence bending stiffness) to the panel sandwich.

Several important dimensional parameters are shown in figure 14. In general, it is desirable to use face sheets (for both the panel and stiffeners) that are as thin as possible. It is feasible to fabricate face sheets that are as thin as .004 inches and this value is assumed for the present discussion. Increasing the face sheet thickness significantly increases panel mass without appreciably improving stiffness. Similarly, it is desirable to keep the width of the stiffener core (0.5 inches in the figure) as small as possible. A stiffener core width of 0.5 inches was selected because it is large enough to prevent stiffener buckling. The remaining dimensional parameters shown in figure 10 are panel core thickness,  $t$ , and stiffener depth,  $d$ . These are important design parameters because they have the greatest impact on overall panel stiffness. The results of analyses involving these parameters are presented later in this section.

Before proceeding, it is useful to discuss how the panels will be attached to the deployable support truss. Truss attachment locations for the two stiffener configurations considered (figure 13) are shown in figure 15. Although both stiffener configurations are compatible with attachment to the 7-panel deployable support truss, configuration 1 is particularly convenient because each attachment location lies at the end of a stiffener. This arrangement provides efficient load transfer from the panel to the underlying truss. Configuration 2 is not as efficient at load transfer, but due to the axisymmetric arrangement of the stiffeners may have advantages for some loading conditions. The panels are attached to the truss using three flexures that provide a statically determinate mounting condition. The flexures restrain panel rotation and out-of-plane motion, but allow for radial expansion as shown in the figure. During thermal expansion of the panels, the flexures allow radial growth, and in so doing reduce surface distortion and thermal load transfer to the support truss. It is noted that analysis results presented in this section assume that the panel attachments are located on the panel perimeter (figure 15). This is in contrast to figure 2, where two of the attachment locations for the seven panel deployable truss are shown inboard of the panel perimeter. Thus, although the results presented are typical and show the important panel trends, they are slightly more conservative (lower predicted stiffness) than those that would be obtained for panels mounted as shown in figure 2.

One measure of panel stiffness and a key structural performance parameter is fundamental frequency. Although specific panel frequency requirements are not presently known, finite element analysis models have been used to determine important frequency trends related to the design variables  $t$  and  $d$  shown in figure 14. Analysis results for fundamental frequency (mode 1) and total panel mass as a function of stiffener depth for each configuration are shown in figure 16. These results assume a panel core thickness of 0.5 inches and a flexure support condition as shown in figure 15. Both configurations exhibit a significant increase in frequency (stiffness) as stiffener depth increases. Furthermore, for stiffener depths less than 4 inches, there is not a great difference between the two panel configurations. The relationship between configurations 1 and 2 is seen more clearly in figure 17 where the ratio of panel frequency to panel mass has been plotted as a function of stiffener depth. The results in the figure show that configuration 2 is slightly more efficient for stiffener depths less than 4 inches. However, as shown in figure 16, mode 1 frequencies

ranging from approximately 13 Hz to 28 Hz are achievable with either stiffener configuration. Both figures 16 and 17 illustrate how stiffeners can be used to increase stiffness without significantly increasing total panel mass, which is less than 5.25 lbm for the entire range of stiffeners plotted on the graphs. The mode shapes associated with the mode 1 frequencies are typical plate bending modes. The leveling off of the frequency curve for configuration 2 is indicative of that configuration's inefficiency in transferring inertial loads to the support points as the mass of the stiffeners is increased.

A more complete understanding of how panel stiffness is related to the design parameters  $t$  and  $d$  is obtained by examination of figure 18. The results in this figure show panel fundamental frequency and mass for a range of panel core thicknesses and stiffener depths, and can be used to determine the lowest mass panel (and associated  $t$  and  $d$ ) that will satisfy a particular frequency requirement. Results are shown for stiffener configuration 1, but the trends are valid for either panel configuration. As stiffener depth increases (following any constant core thickness curve), there is a significant increase in frequency (stiffness) and a correspondingly small increase in mass. Conversely, as panel core thickness is increased (following a constant stiffener depth curve), there is a small increase in frequency and a correspondingly large increase in mass. Thus, as expected, adding depth to the panel stiffeners improves performance more efficiently than adding thickness to the panel core. The abrupt curvature at the left side of each constant core thickness curve indicates that shallow stiffeners are relatively inefficient.

It can be seen from figure 18 that the lowest mass panel satisfying a specific frequency requirement is obtained by selecting the thinnest possible panel core and adding stiffeners of sufficient depth. A reasonable lower limit for panel core thickness is 0.25 inch, represented by the lowest curve in figure 18. However, packaging requirements may place a constraint on allowable total panel thickness, and thus may preclude the use of the "thinnest core" and "lowest mass" panel. For example, a panel frequency requirement of 20 Hz can be satisfied using a panel having a core thickness of 0.25 inches and stiffeners having a depth of approximately 3.4 inches. The total panel thickness for this example is 3.658 inches (3.4 inches + .25 inches + two face sheets), and the panel mass is approximately 3.75 lbm. If, for example, a packaging constraint requires that the total thickness be no more than 3.0 inches, the same frequency requirement (20 Hz) can be satisfied only with a thicker panel core. Figure 19 is a modification of figure 18, with the parameter "total panel thickness" exchanged for the parameter "stiffener depth". The results in figure 19 show that for a maximum allowable total thickness of 3.0 inches, a frequency requirement of 20 Hz dictates a core thickness of approximately 0.65 inch (and thus stiffeners with depth 2.35 inches). The resulting panel has a mass of approximately 5.0 lbm, an increase of 33% from that of the "thinnest core" panel.

The results in figures 18 and 19 provide a panel design tool that may be useful for a relatively wide range of possible core thicknesses and stiffener depths, and for a variety of possible reflector applications and potential launch vehicles. However, the assumptions for the reflector design of the present paper limit the total panel thickness to 2.0 inches. Figure 19 shows that for this total thickness value, a frequency of approximately 12 Hz is obtained using a panel with a 0.25 inch core (1.75 in. stiffeners) and a mass of 3.3

lbm. This mass value does not include the mass of any additional hardware used to attach the panel to the support truss. Alternatively, a slightly more massive panel having a core of 0.50 inches and no stiffeners achieves a frequency of approximately 14 Hz. Although not the most efficient, such a panel has the advantage that it is thinner (.508 inch total) and enables packaging of a feed boom with a larger cross section for increased dynamic performance. Although the panel with no rib stiffeners is easier to fabricate its mass is increased to approximately 3.9 lbm. Figure 19 also indicates that with a total panel thickness limit of 2.0 inches, frequencies greater than 12 Hz can be obtained only by using thicker core panels that are significantly more massive. For example, a frequency requirement of 20 Hz requires a panel having mass greater than 5 lbm, and a requirement of 30 Hz cannot be obtained for the range of stiffener core thicknesses shown in figure 15.

This section has described two rib-stiffened panel configurations and presented analytical results for mass and stiffness. The important design variables have been examined. The results show that the addition of only a few sufficiently deep rib stiffeners can efficiently improve sandwich panel stiffness. The best panel design for the 7-panel deployable reflector of this paper must still be determined. The effects of thermal distortion and issues related to surface accuracy, panel fabrication, compact packaging, and costs must still be addressed. In addition, assuming fabrication cost is not significantly affected, it may be useful to investigate alternative panel designs that utilize more stiffeners. For example, configurations using more than three stiffeners might show significantly improved performance even when shallow stiffeners are mandated by panel packaging requirements.

#### Concluding Remarks

A concept is presented for achieving a remotely deployable reflector with an integrated feed boom that has potential for meeting aperture size and surface precision requirements for some high-frequency microwave remote sensing applications and which, in packaged form, can be conveniently attached as a unit to a spacecraft bus.

The non-deployable center section of the support truss enables simple attachment of the self-contained packaged reflector unit to a spacecraft bus. Although the basic sequence of motions necessary to deploy the reflector and feed boom are shown conceptually to be feasible, the details of the linkages, actuators, fittings, latches, etc. to cause these motions, maintain the proper deployed configuration, and support the package for survival of launch loads could have significant impact on mass, package size, and deployment complexity.

A reflector having a focal length of 216 inches and consisting of seven 80-inch-diameter panels can be sized to fit within the Space Shuttle cargo bay using the MPSS as the mounting pallet. The reflector and feed boom can be deployed while remaining attached to the MPSS in the Space Shuttle cargo bay. With reversible actuators, a refolding capability is possible to enable a Shuttle flight experiment that could be used to verify reliability of deployment through multiple deployment testing.

Analysis of the reflector sized for Space Shuttle transportation shows that the feed boom and spacecraft bus can have a significant impact on the fundamental frequency of the deployed configuration. The fundamental frequency of an unsupported reflector dish (7 panels and support truss) is reduced by a factor of 3 when the feed boom is included in the model. In addition, increasing the mass of a spacecraft bus in the model further reduces the fundamental frequency. As the spacecraft bus mass is increased, the boundary conditions on the spacecraft bus end of the reflector structure (at the base of the center-body truss) approach a clamped condition, resulting in a significant degradation of the fundamental frequency. A Space Shuttle flight experiment wherein the deployed reflector would remain firmly attached to a support pallet in the cargo bay would experience this degradation in fundamental frequency.

Analyses of two candidate panel configurations for deployable reflector application show that sandwich panel stiffness can be more efficiently increased by the addition of only a few sufficiently deep ribs than by increasing the core depth. The best panel design for the 7-panel reflector concept presented herein must still be determined. The effects of thermal distortion and issues related to surface accuracy, panel fabrication, compact packaging, and costs must still be addressed. It may be useful to investigate alternative panel designs that utilize more than three stiffeners. Consideration of the advantages must be weighed against fabrication costs, however, since the addition of stiffeners may increase the complexity of fabrication.

#### References

1. Carsey, Frank D., editor: Microwave Remote Sensing of Sea Ice. Geophysical Monograph 68, American Geophysical Union, 1992.
2. Campbell, T. G., Lawrence, R. W., Schroeder, L. C., Kendall, B. M., and Harrington, R. F.: Development of Microwave Radio Sensor Technology for Geostationary Earth Science Platforms. IGARSS '91, Remote Sensing: Global Monitoring for Earth Management, 1991 International Geoscience and Remote Sensing Symposium, vol. II. IEEE Catalog No. 91CH2971-0, Lib. of Congress No. 90-86187.
3. Hedgepeth, John M.: Structures for Remotely Deployable Precision Antennas. NASA CR 182065, Jan. 1989.
4. Mikulas, Martin M., Jr.; Freeland, Robert F., and Taylor, Robert M.: One-Ring Deployable High Precision Segmented Reflector Concept. JPL D-9845, June 1992.
5. Wu, K. Chauncey and Sutter, Thomas R.: Structural Analysis of Three Space Crane Articulated-Truss Joint Concepts. NASA TM 4373, May 1992.



6. Hitchhiker--Customer Accommodations & Requirements Specifications (CARS). HHG-730-1503-06, Goddard Space Flight Center, Greenbelt, Md. 1992.
7. Whetstone, W. D.: EISI-EAL Engineering Analysis Language Reference Manual - EISI-EAL System 312. Engineering Information Systems, Inc., Aug. 1985.

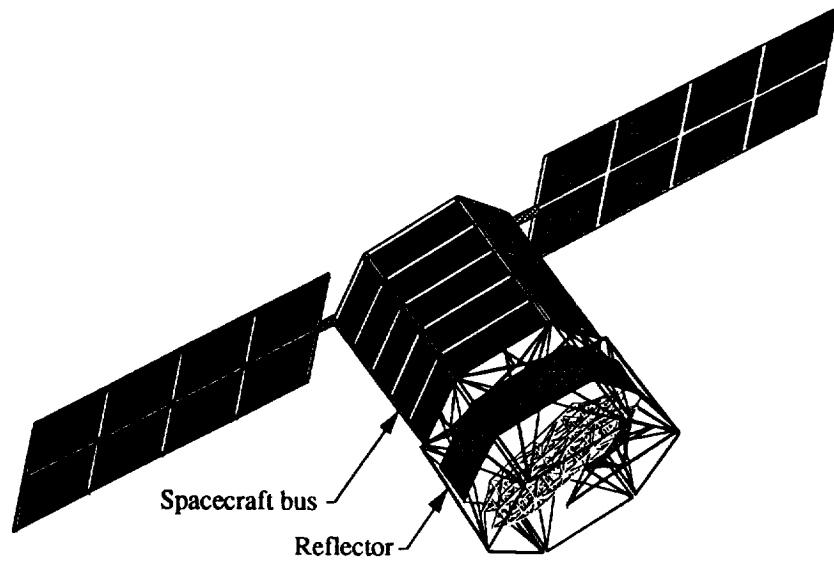
Table 1. Mass of non-structural components.

Item	Quantity	Mass, lbm Per Item	Total Mass, lbm
Panels	7	5.00	35.00
Actuators on Center-Body Truss	6	0.25	1.50
Actuators on Wings	12	0.38	4.50
Actuators in Feed Boom	2	0.50	1.00
Physical Nodes	115	0.10	11.50
Total Non-Structural Mass			53.50

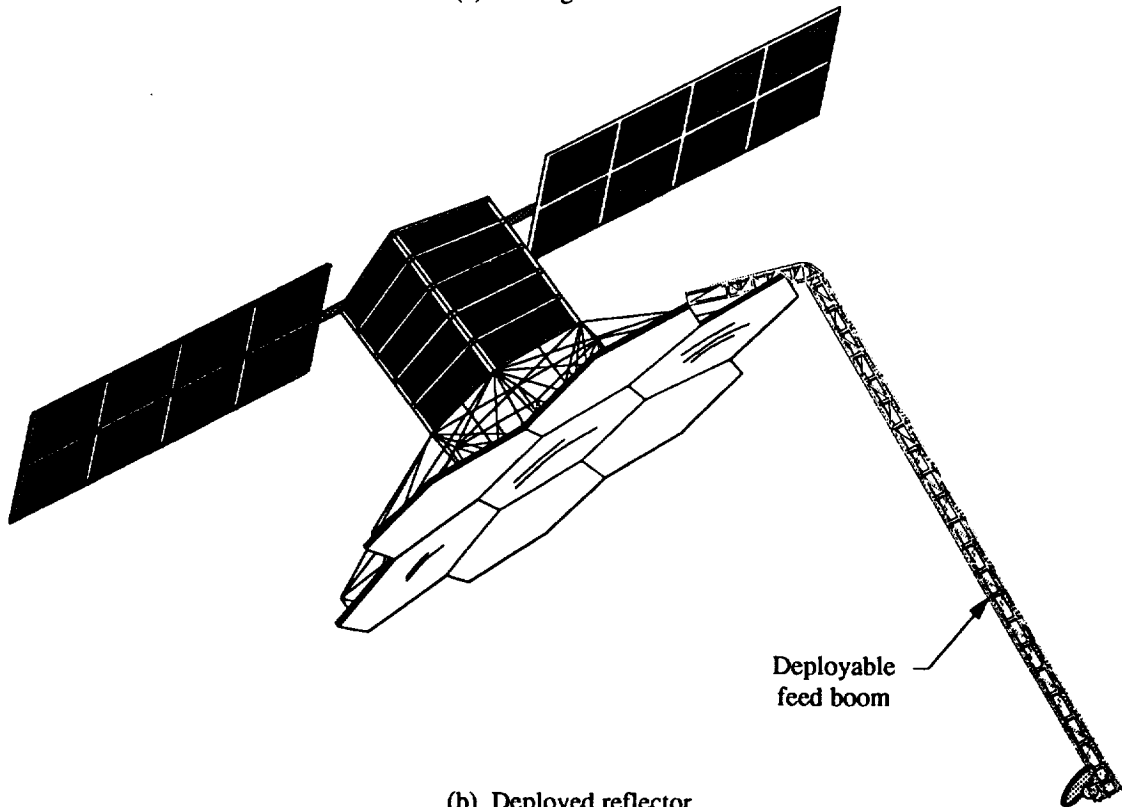
Table 2. First two frequencies for various feed and spacecraft bus masses.

Mass, lbm		Frequency, Hz	
Feed	Spacecraft Bus	Fundamental	2nd
0	0	8.44 (T)	8.84 (B)
2	0	7.64 (T)	7.68 (B)
5	0	6.74 (B)	7.15 (T)
10	0	5.99 (B)	6.76 (T)
20	0	5.29 (B)	6.46 (T)
0	350	6.75 (T)	7.66 (B)
2	350	5.85 (T)	6.50 (B)
5	350	5.21 (T)	5.58 (B)
10	350	4.70 (B)	4.87 (T)
20	350	4.13 (B)	4.35 (T)
0	700	6.27 (T)	7.17 (B)
2	700	5.35 (T)	6.06 (B)
5	700	4.69 (T)	5.18 (B)
10	700	4.16 (T)	4.48 (B)
20	700	3.70 (B)	3.82 (T)
0	1400	5.83 (T)	6.67 (B)
2	1400	4.90 (T)	5.60 (B)
5	1400	4.20 (T)	4.75 (B)
10	1400	3.64 (T)	4.06 (B)
20	1400	3.17 (T)	3.42 (B)

(T) twisting  
(B) bending



(a) Packaged reflector



(b) Deployed reflector

Figure 1. Schematic of segmented precision reflector attached to spacecraft bus.

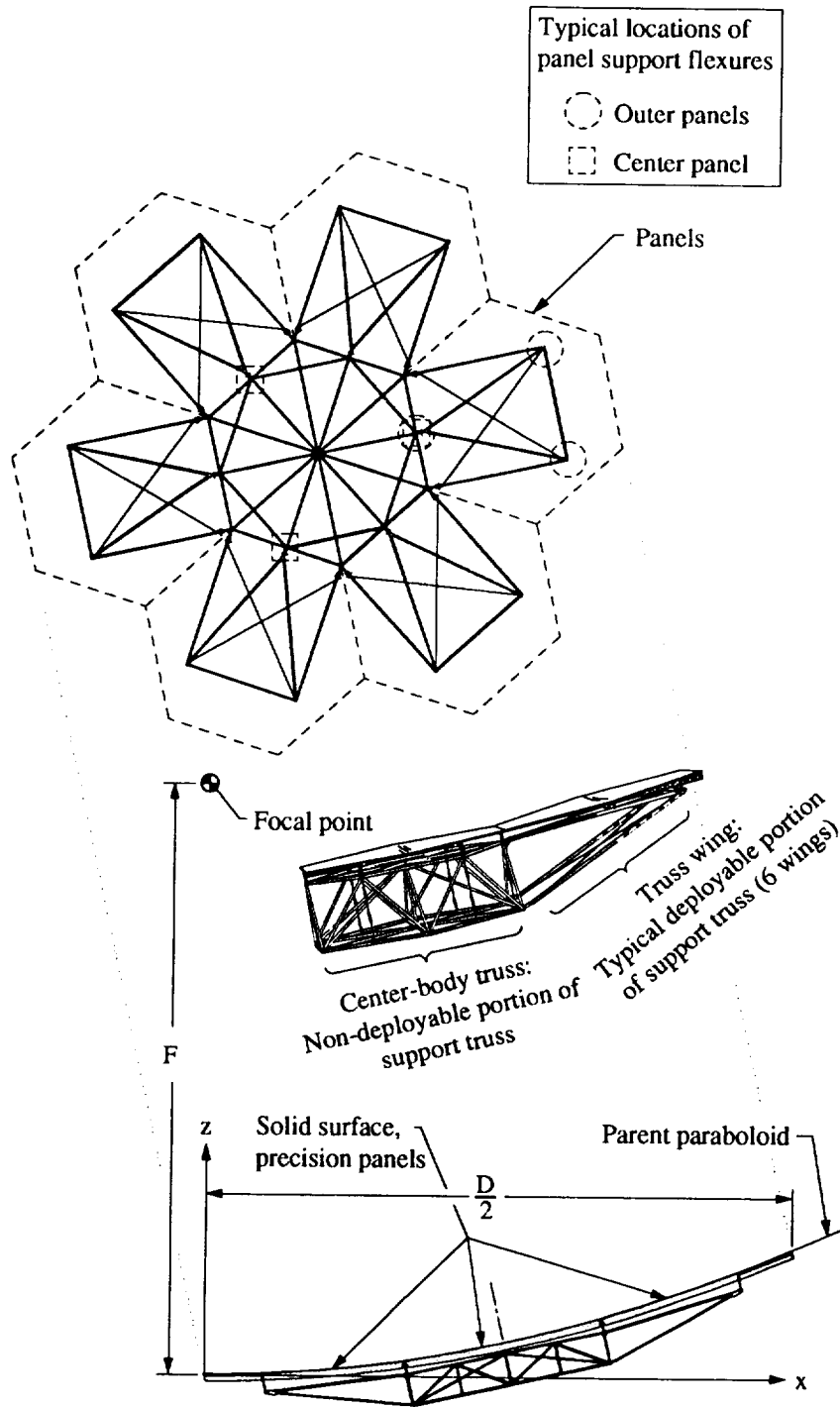


Figure 2. Offset parabolic reflector geometry.

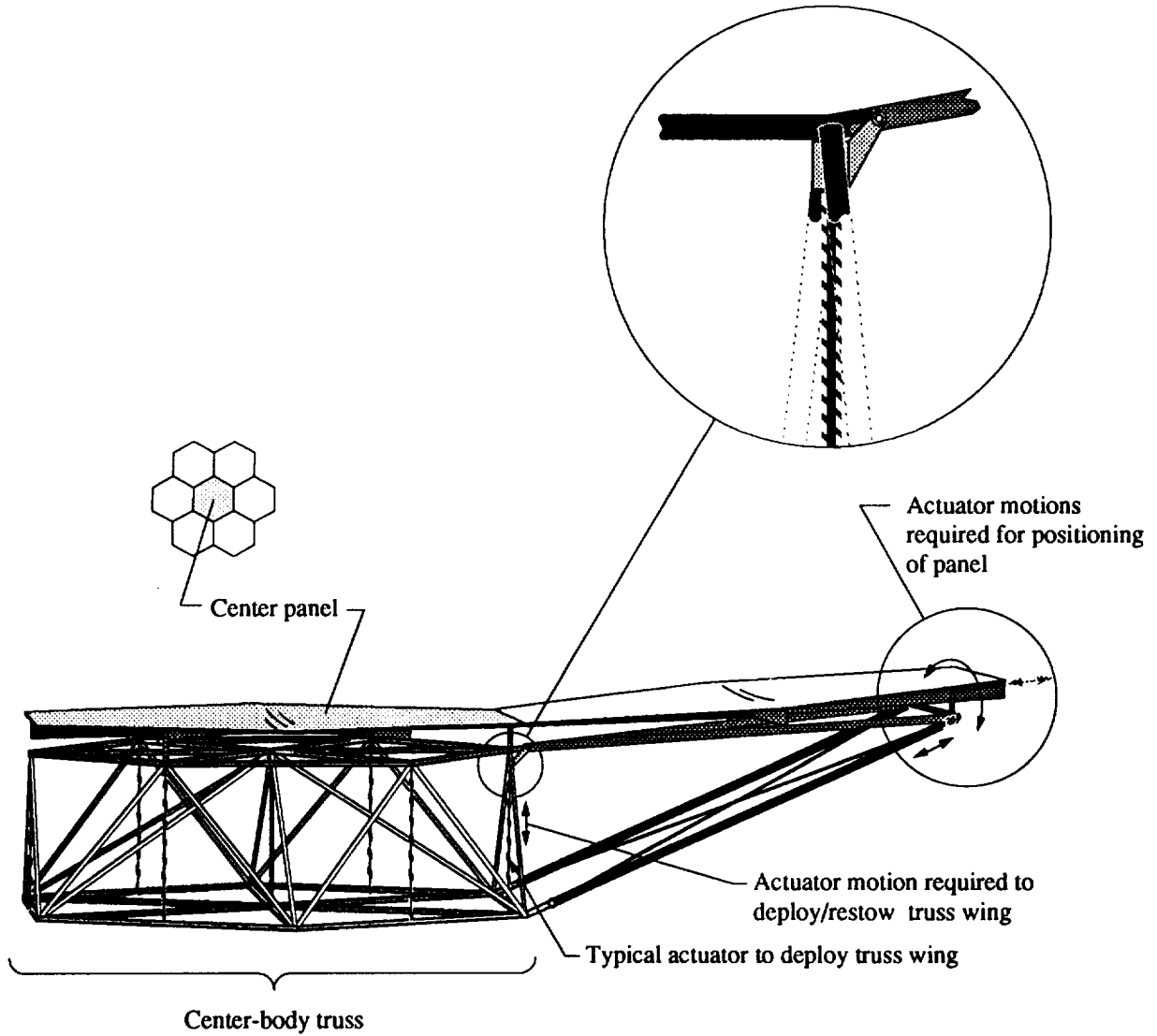
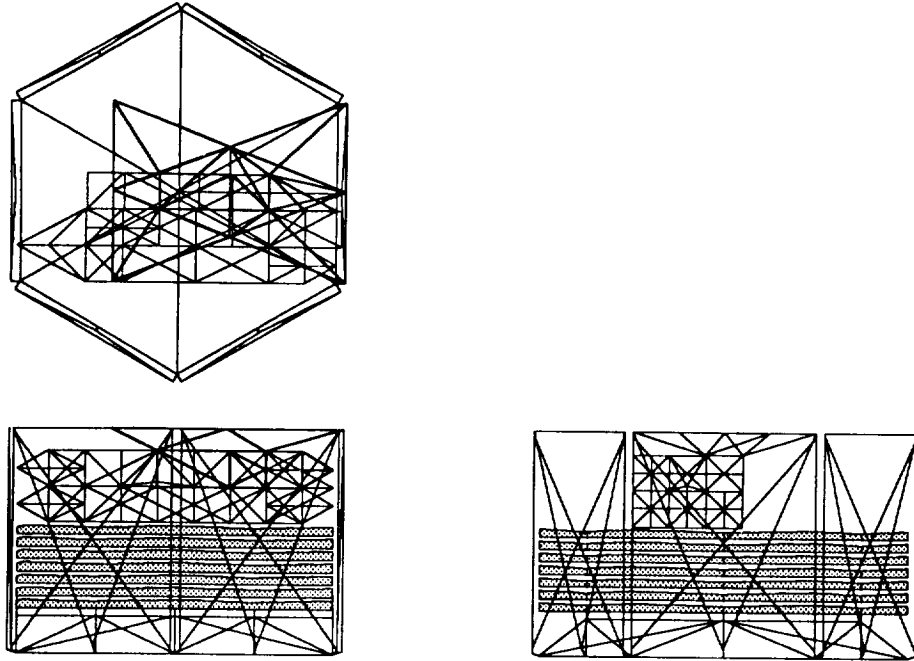
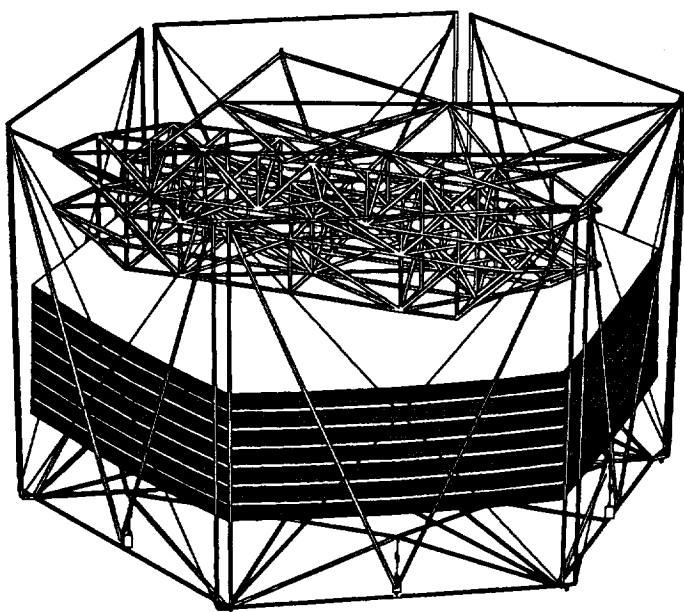


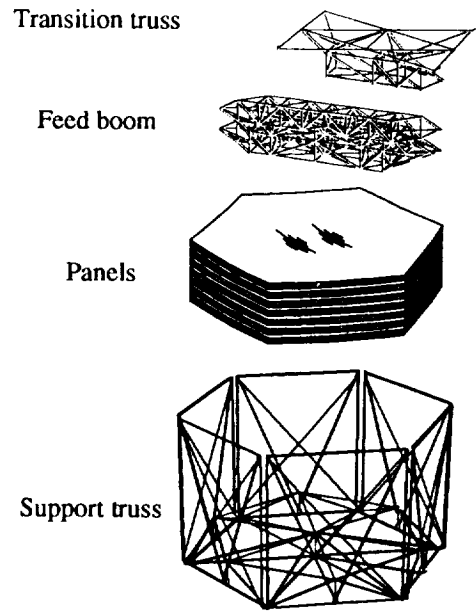
Figure 3. Perspective view showing center-body truss with attached center panel and one wing of the reflector in the deployed configuration.



(a) Orthographic projection



(b) Perspective view



(c) Components

Figure 4. Packaged configuration of 7-panel reflector.

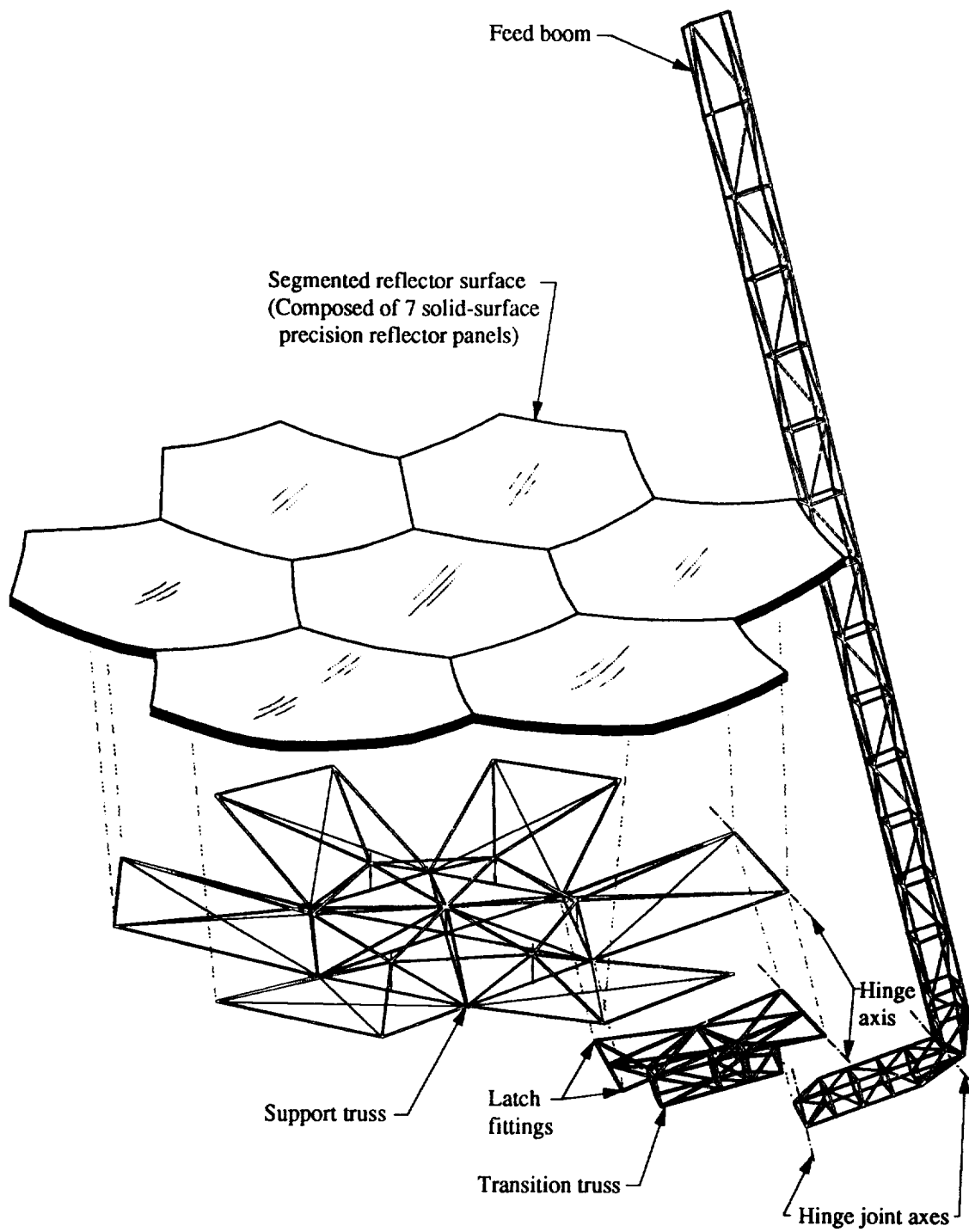
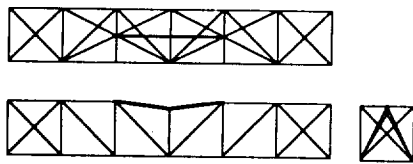
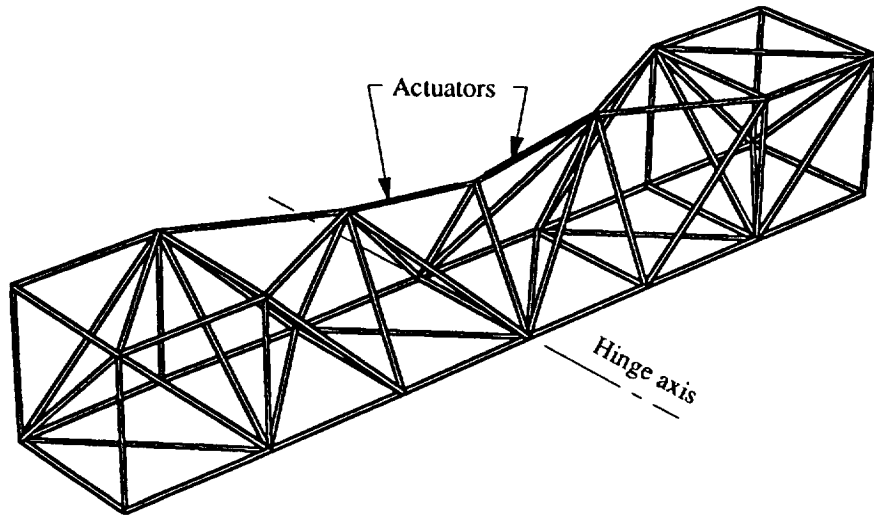
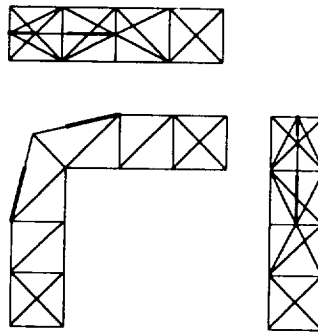


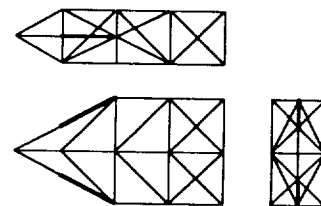
Figure 5. Exploded view of deployed 7-panel reflector.



(a) Straight configuration



(b) 90° bend



(c) 180° bend

Figure 6. Feed boom hinge joint. (Joint concept A, Ref. 5)

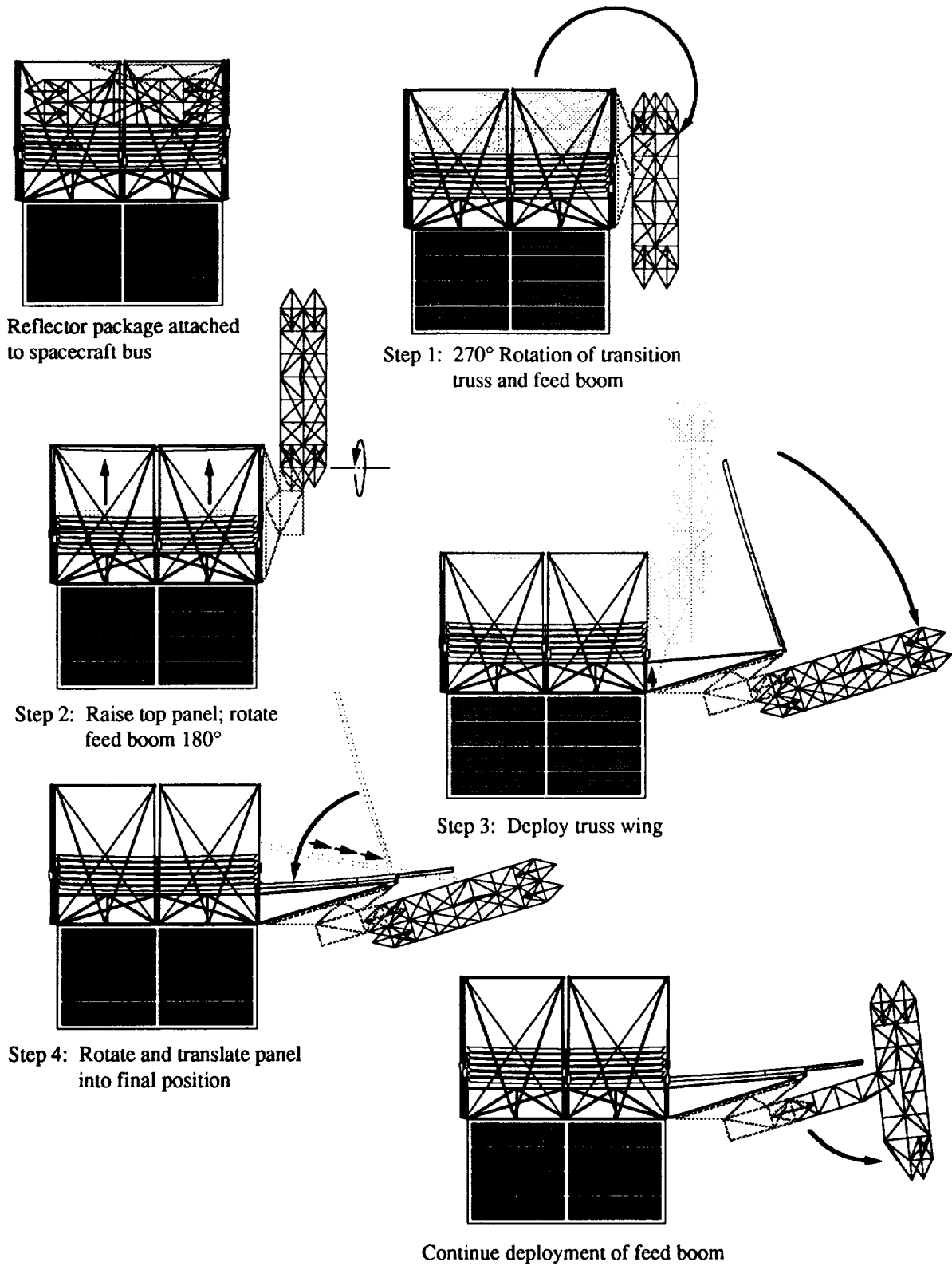


Figure 7. Schematic showing deployment of top panel and feed boom when reflector is attached to a spacecraft bus.



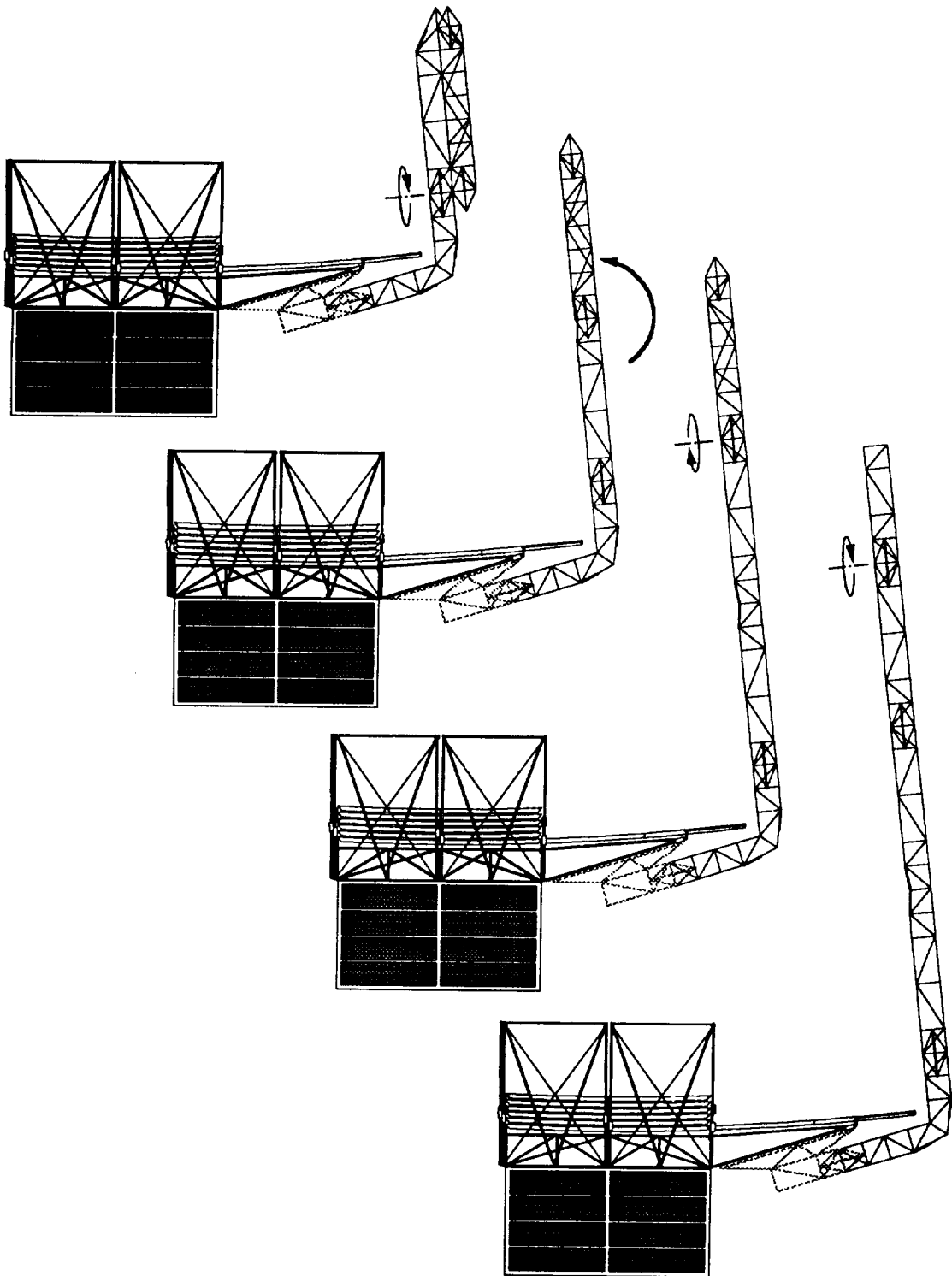


Figure 7. Concluded

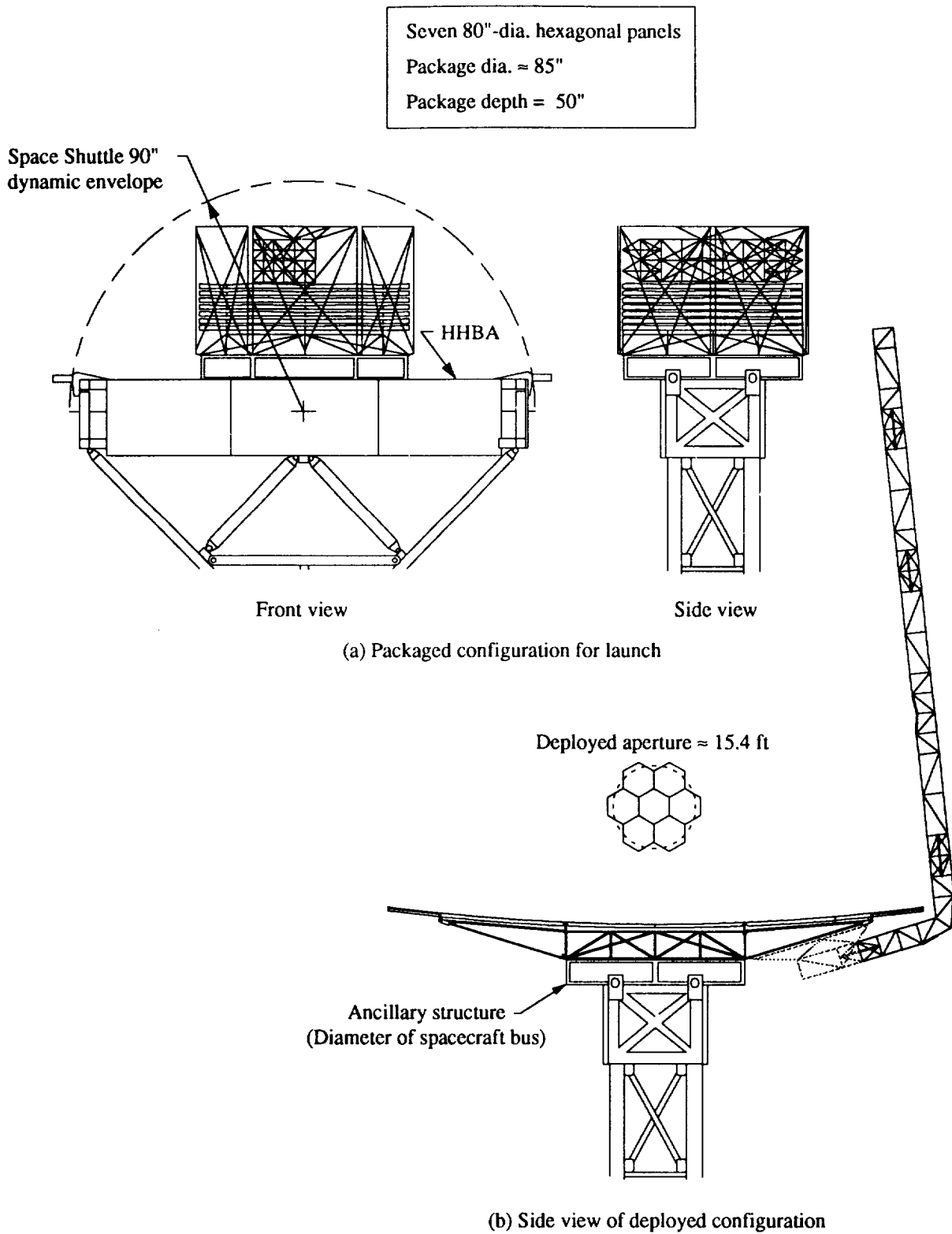
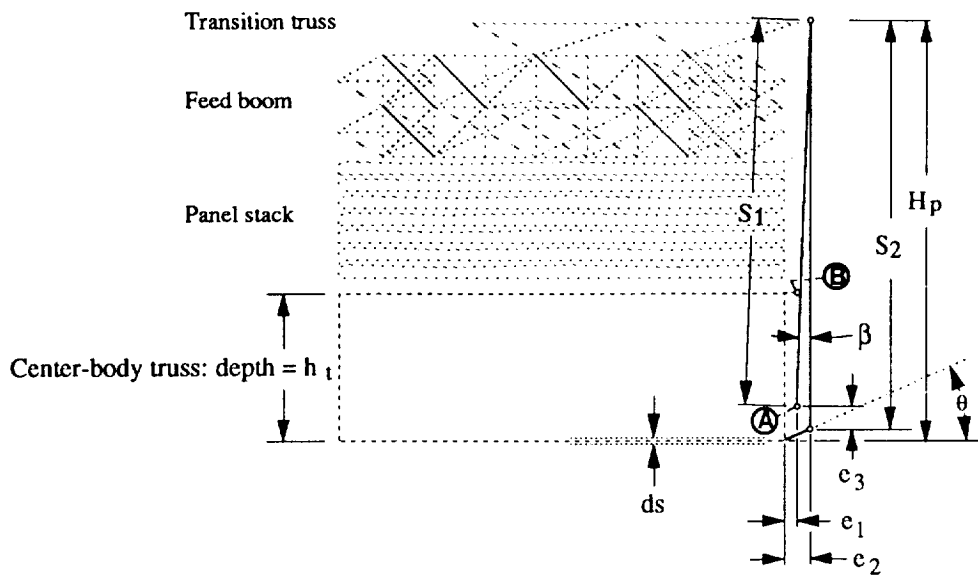
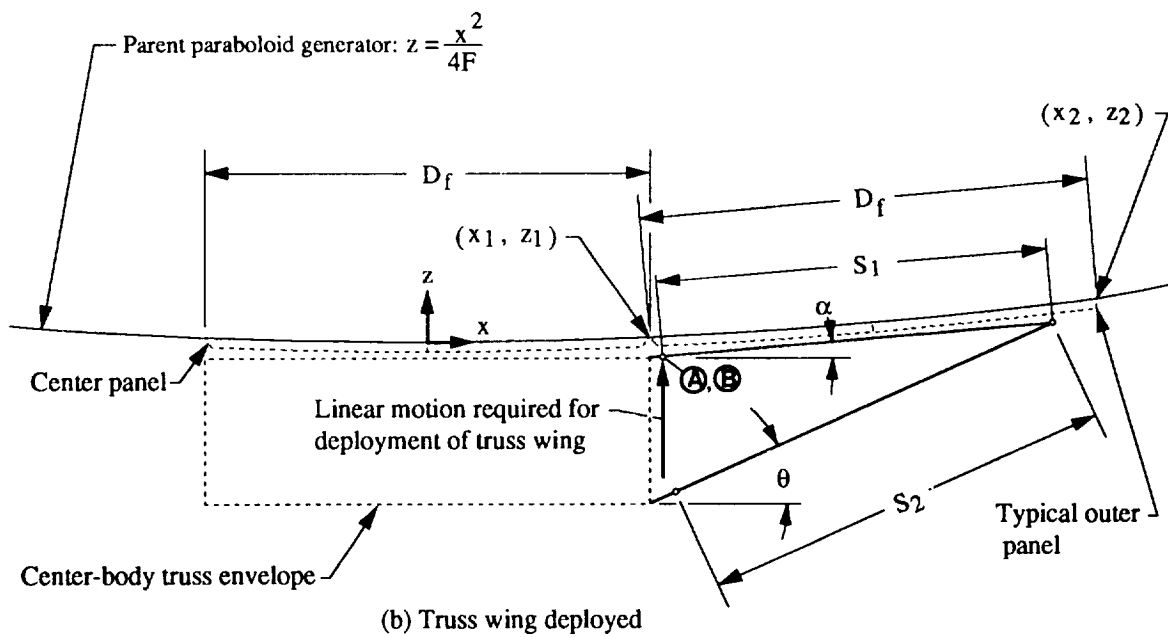


Figure 8. Truss-stiffened 7-panel deployable reflector attached to the Hitchhiker Bridge Assembly (HHBA) in the Space Shuttle cargo bay.



(a) Truss wing folded



(b) Truss wing deployed

Figure 9. Truss geometry

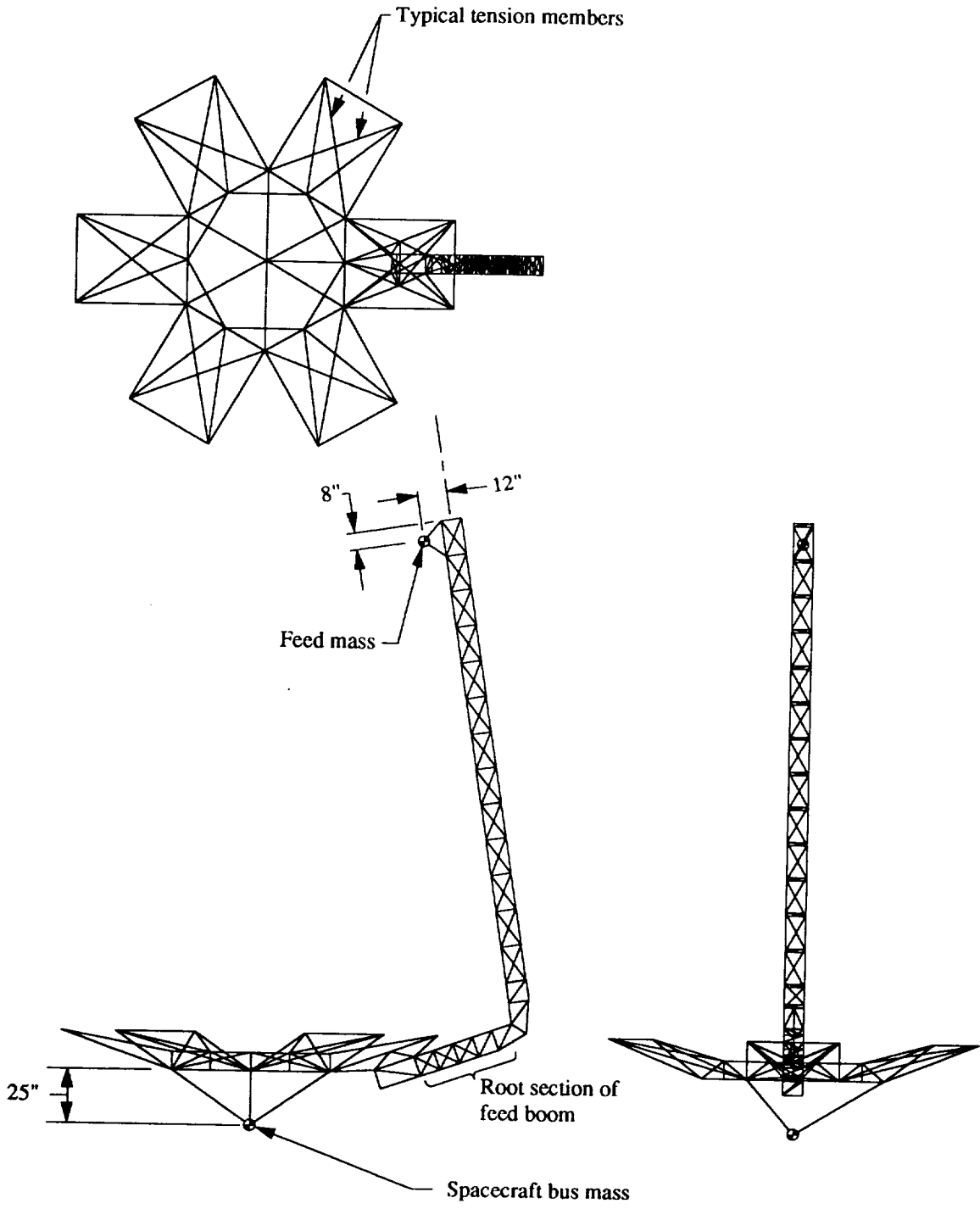
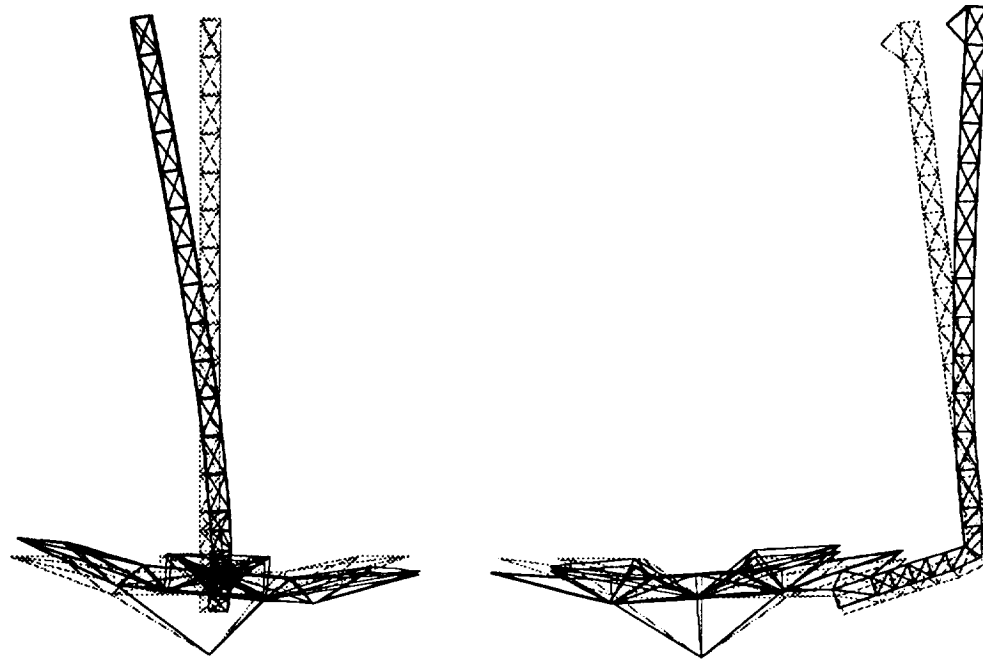


Figure 10. Finite-element model.



(a) Mode referred to as "twisting mode"      (b) Mode referred to as "bending mode"

Figure 11. Typical modes of vibration for the two lowest natural frequencies.

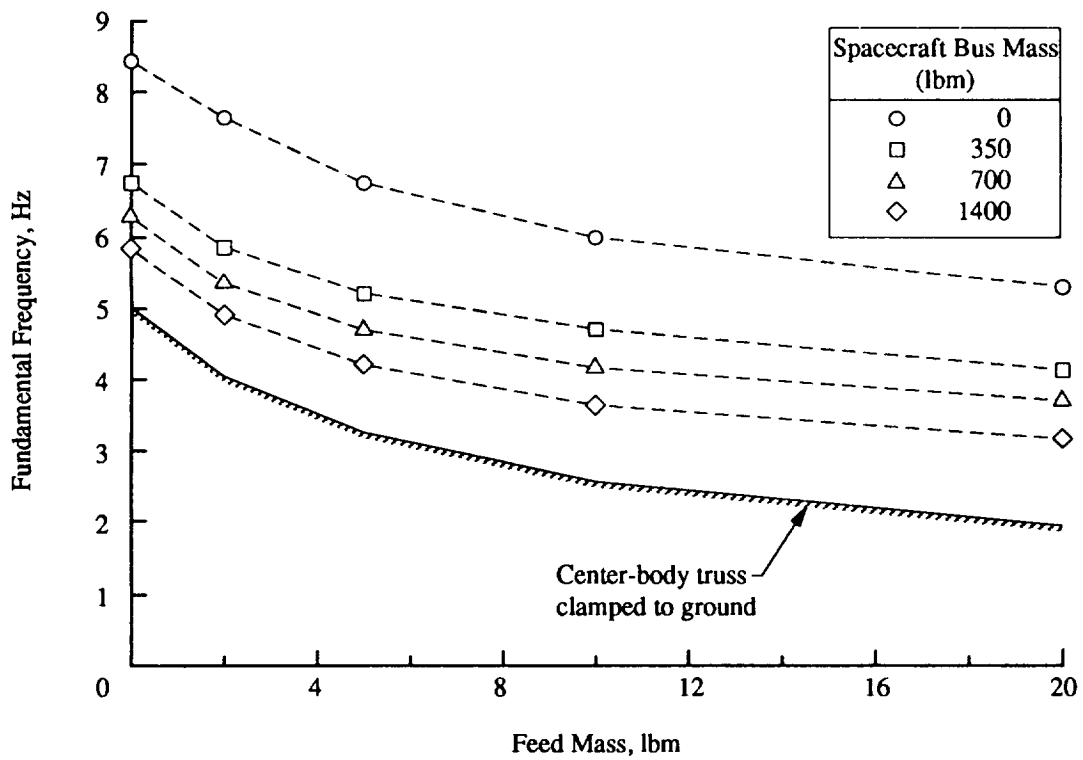


Figure 12. Effect of feed mass and spacecraft mass on fundamental frequency.

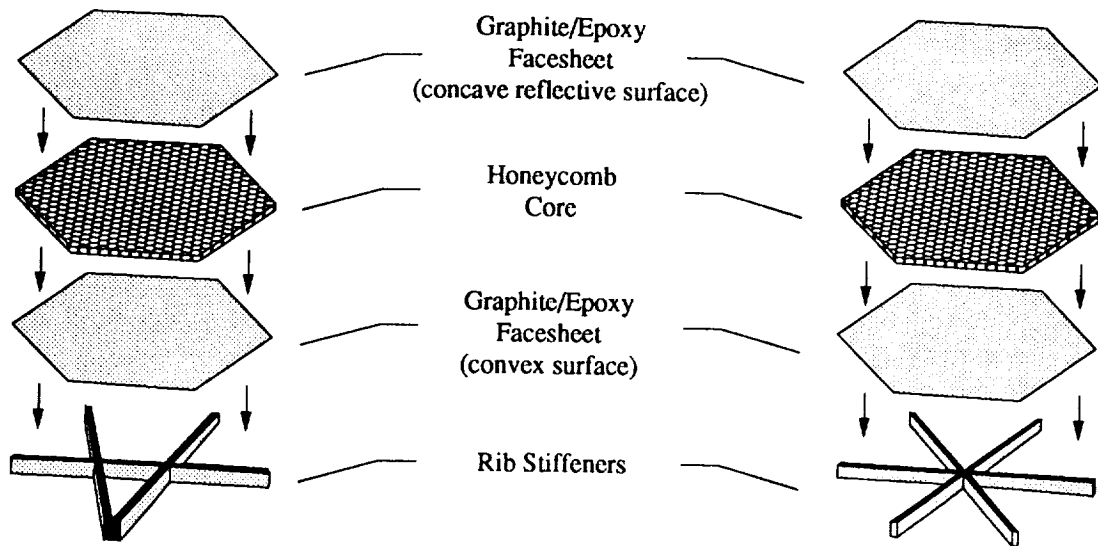


Figure 13. Rib stiffened lightweight deployable reflector panel concepts.

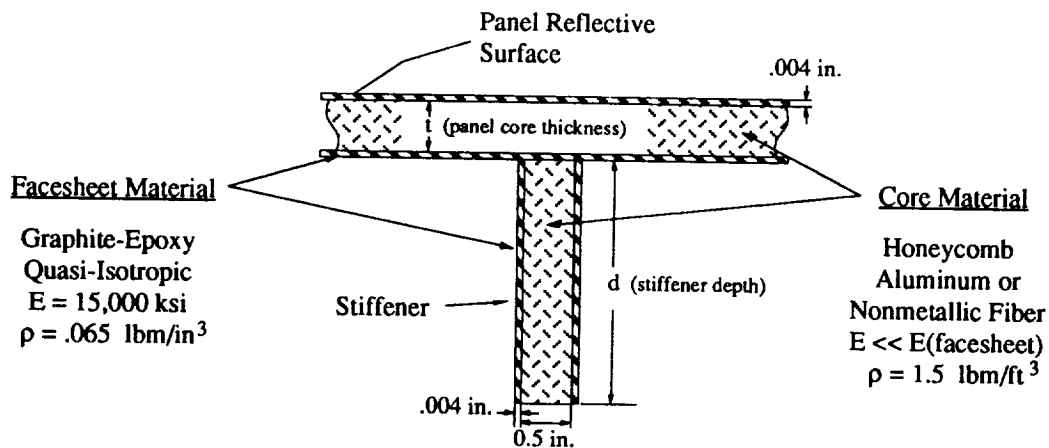


Figure 14. Cross section of typical panel and stiffener.

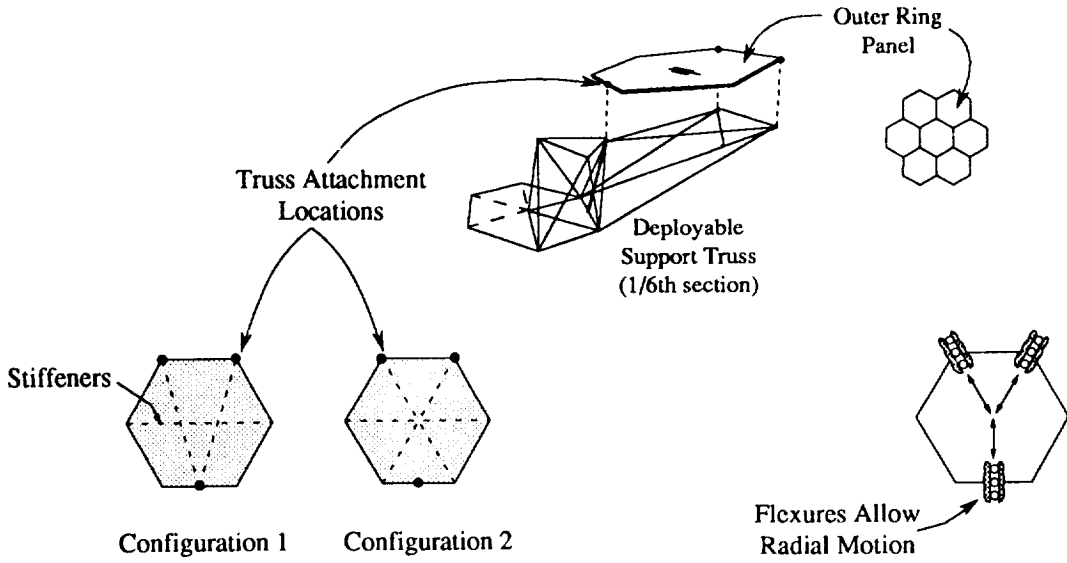


Figure 15. Attachment of outer ring panels to deployable support truss.

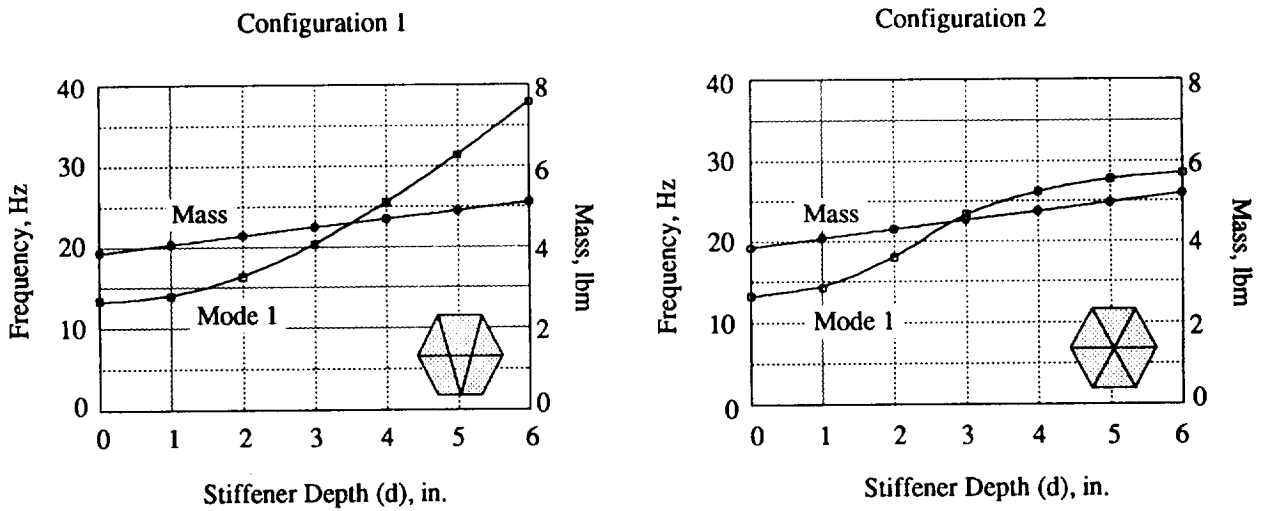


Figure 16. Mode 1 frequency and panel mass as a function of stiffener depth. (panel core thickness,  $t = 0.5$  in.)

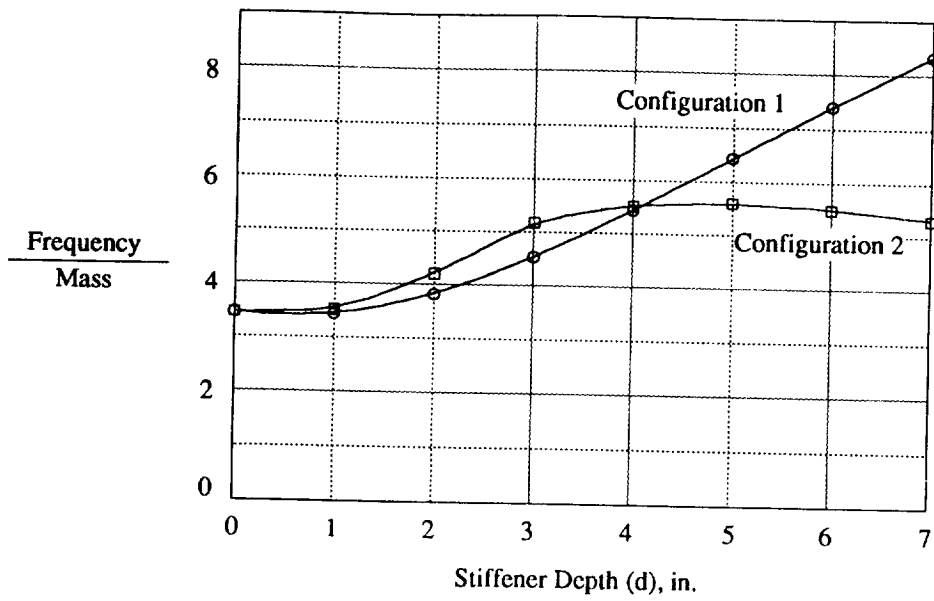


Figure 17. Frequency to mass ratios as a function of stiffener depth for configurations 1 and 2 (panel core thickness,  $t = 0.5$  in.)

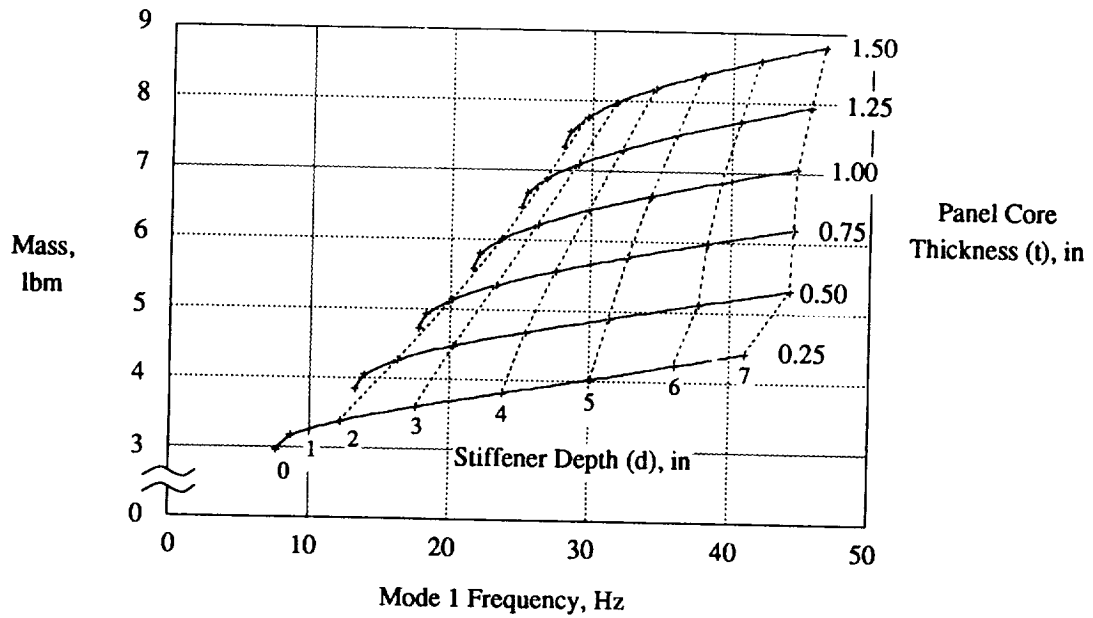


Figure 18. Mode 1 frequency and panel mass as a function of core thickness and stiffener depth (stiffener configuration 1)



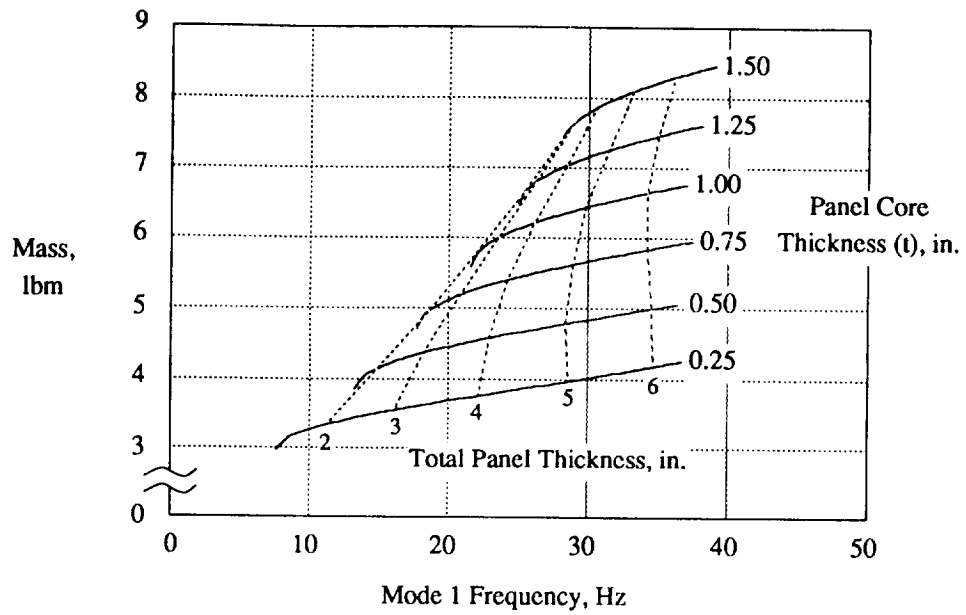


Figure 19. Mode 1 frequency and panel mass as a function of core thickness and total panel thickness (stiffener configuration 1)

# REPORT DOCUMENTATION PAGE

*Form Approved*  
OMB No. 0704-0188

Public reporting burden for this collection of information is estimated to average 1 hour per response, including the time for reviewing instructions, searching existing data sources, gathering and maintaining the data needed, and completing and reviewing the collection of information. Send comments regarding this burden estimate or any other aspect of this collection of information, including suggestions for reducing this burden, to Washington Headquarters Services, Directorate for Information Operations and Reports, 1215 Jefferson Davis Highway, Suite 1204, Arlington, VA 22202-4302, and to the Office of Management and Budget, Paperwork Reduction Project (0704-0188), Washington, DC 20503.

<b>1. AGENCY USE ONLY (Leave blank)</b>		<b>2. REPORT DATE</b> November 1993	<b>3. REPORT TYPE AND DATES COVERED</b> Technical Memorandum	
<b>4. TITLE AND SUBTITLE</b> Packaging, Deployment, and Panel Design Concepts for a Truss-Stiffened 7-Panel Deployable Precision Reflector with Feed Boom			<b>5. FUNDING NUMBERS</b> WU 506-43-41-02	
<b>6. AUTHOR(S)</b> Walter L. Heard, Jr.; Timothy J. Collins; James W. Dyess; W. Scott Kenner; and Harold G. Bush				
<b>7. PERFORMING ORGANIZATION NAME(S) AND ADDRESS(ES)</b> NASA Langley Research Center Hampton, VA 23681-0001			<b>8. PERFORMING ORGANIZATION REPORT NUMBER</b>	
<b>9. SPONSORING / MONITORING AGENCY NAME(S) AND ADDRESS(ES)</b> National Aeronautics and Space Administration Washington, DC 20546-0001			<b>10. SPONSORING / MONITORING AGENCY REPORT NUMBER</b> NASA TM-109000	
<b>11. SUPPLEMENTARY NOTES</b>				
<b>12a. DISTRIBUTION / AVAILABILITY STATEMENT</b> Unclassified - Unlimited  Subject Category - 18			<b>12b. DISTRIBUTION CODE</b>	
<b>13. ABSTRACT (Maximum 200 words)</b> A concept is presented for achieving a remotely deployable truss-stiffened reflector with seven integrated sandwich panels and feed boom that has potential for meeting aperture size and surface precision requirements for some high-frequency microwave remote sensing applications. The package reflector/feed boom configuration is a self contained unit that can be conveniently attached to a spacecraft bus. The package has a cylindrical envelope compatible with typical launch vehicle shrouds. Dynamic behavior of the deployed configuration consisting of 80-inch-diameter, two-inch thick panels and a 224 inch feed boom is examined through finite-element analysis.				
<b>14. SUBJECT TERMS</b> Deployable Reflector; Precision Segmented Reflector; Feed Boom; Sandwich Panels			<b>15. NUMBER OF PAGES</b> 32	
			<b>16. PRICE CODE</b> A03	
<b>17. SECURITY CLASSIFICATION OF REPORT</b> Unclassified	<b>18. SECURITY CLASSIFICATION OF THIS PAGE</b> Unclassified	<b>19. SECURITY CLASSIFICATION OF ABSTRACT</b> Unclassified	<b>20. LIMITATION OF ABSTRACT</b>	